Electrically Pumped Vertical External Cavity Surface Emitting Lasers Suitable for Passive Modelocking

Yohan Barbarin, M. Hoffmann, W. P Pallmann, I. Dahhan, P. Kreuter, M. Miller, J. Baier, H. Moench, M. Golling, T. Südmeyer, et al.

Electrically Pumped Vertical External Cavity Surface Emitting Lasers Suitable for Passive Modelocking

Y. Barbarin, M. Hoffmann, W. P. Pallmann, I. Dahhan, P. Kreuter, M. Miller, J. Baier, H. Moench, M. Golling, T. Südmeyer, B. Witzigmann and U. Keller.

***Abstract*— Modelocked optically pumped vertical external-cavity surface emitting lasers (VECSELs) have generated up to 6.4 W average power, which is higher than for any other semiconductor lasers. Electrical pumping (EP) of modelocked VECSELs is the next step towards a higher level of integration. With continuous wave (cw) EP-VECSELs an average output power of 900 mW has been demonstrated from the undisclosed proprietary NECSEL design. In contrast, modelocked NECSELs have only been demonstrated at 40 mW. Recently, we presented a numerical study of EP-VECSELs suitable for modelocked operation, here we demonstrate the first realization of this design. Power scaling is achieved with a lateral mode size increase. The competing electrical and optical requirements are, on the electrical side, low ohmic resistance, and on the optical side, low optical losses and low dispersion. Additionally, the device needs to operate in a fundamental mode for stable modelocking. We have fabricated and characterized 60 EP-VECSELs with varying dimensions and compared their lasing performance with our numerical simulations. The trade-off between good beam quality and output power is discussed with an outlook to the modelocking of these EP-VECSELs. Initial EP-VECSEL devices have generated >100 mW of cw output power.**

***Index Terms*— Semiconductor lasers, vertical emitting lasers, Modelocked lasers, optoelectronic devices.**

Manuscript received Dec. 1st, 2010. This work was supported by ETH Zurich with the FIRST cleanroom facility and was financed by the Intel Corporation through a university sponsored research agreement, by the Swiss Confederation Program Nano-Tera.ch which was scientifically evaluated by the SNSF and by the European Community's Seventh Framework Program FAST-DOT under grant agreement 224338.

Y. Barbarin, M. Hoffmann, W. P. Pallmann, I. Dahhan, M. Golling, T. Südmeyer, and U. Keller are from the department of Physics, Institute for Quantum Electronics, at ETH Zurich, Switzerland. (e-mails: barbarin@phys.ethz.ch and keller@phys.ethz.ch).

P. Kreuter and B. Witzigmann were from the Department of Information Technology and Electrical Engineering, Integrated Systems Laboratory, ETH Zurich, Switzerland.

M. Miller is from Philips Technologie GmbH U-L-M Photonics, Lise-Meitner-Str. 13, 89081 Ulm, Germany.

H. Moench and J. Baier are from Philips Research Laboratories, Weisshausstrasse 2, 52066 Aachen, Germany.

B. Witzigmann and I. Dahhan are from the department of Electrical Engineering and Computer Science, Computational Electronics and Photonics Group, University of Kassel, Germany.

I. Introduction

TODAY, the modelocked laser market is dominated by optically pumped solid-state lasers with an intra-cavity component for pulse formation [1]. Their large size, high cost and complexity limit their commercial use in numerous applications such as displays, biomedical imaging or optical clocking of multi-core processors. Semiconductor lasers constitute a breakthrough technology in optical telecommunications [2], modelocked semiconductor lasers have now the potential to replace solid-state lasers in many applications where high power is required. To date, modelocked edge-emitting lasers (EEL) generate average output powers of up to 250 mW in picosecond pulses [3]. In these devices, the mono-mode waveguide limits the lateral scaling, and in addition, the long light interaction in the waveguide introduces significant dispersion, nonlinearities and noise. It is very challenging to increase the output power of ultrafast EELs to the Watt regime. It can be realized with an additional tapered amplifier and an external pulse compression scheme like in [4], but it significantly complicates the laser cavity and makes the use of semiconductor diodes less attractive.

Vertical external cavity surface emitting lasers (VECSELs) [5] offer excellent beam quality and high output power in the multi-Watt level directly from the resonator. The simple VECSEL external cavity geometry and the use of semiconductor materials allow for cheap mass production and enables passive modelocking of these devices [6] using a semiconductor saturable absorber mirror (SESAM [7]). The SESAM can even be integrated directly in the VECSEL structure. This new type of laser is called a modelocked integrated external-cavity **s**urface emitting laser (MIXSEL) [8-10]. Optically pumped (OP) VECSELs and MIXSELs have generated shorter pulses and higher average powers than any other modelocked semiconductor laser (i.e. 135 fs pulses at 35 mW average power [11], 210 fs pulses at 11 mW [12], 2.1 W in 4.7 ps pulses [13] and 6.4 W in 25 ps pulses from a MIXSEL [10]). Furthermore, modelocked VECSELs have much better noise performance compared to modelocked edge-emitters because of their short light interaction length

and their high-Q cavity [14].

Electrical pumping (EP) of modelocked VECSELs is an important step towards high-power ultrafast compact laser sources. In 2003, Novalux Corporation reported a continuous-wave (cw) output power of 900 mW from their proprietary EP-VECSEL, referred to as the NECSEL [15, 16]. A different approach reported in 2007 by OSRAM consisted of monolithically integrating pump diodes through the VECSEL structure. With such a structure 600 mW of output power in cw operation was obtained [17] but the coupling between the pump laser cavities and the VECSEL gain is quite challenging. In addition, the pumped spot on the VECSEL gain is not necessarily uniform [18]. EP-VECSELs have also been demonstrated at 1.55 µm [19, 20] and 2.3 µm [21] wavelengths, but the difficulties encountered with the distributed Bragg reflectors (DBRs) at those wavelengths currently limit the cw power to the milliwatt level.

The first modelocked EP-VECSEL was reported in 1993 with active modelocking producing 80 ps pulses using a liquid-nitrogen cooled vertical cavity surface emitting laser (VCSEL) structure [22]. Passively modelocked EP-VECSELs have, to our knowledge, only been reported using NECSEL chips. Modelocked operation has been demonstrated with 40 mW of average power in 57 ps pulses [23]. Pulses as short as 15 ps have also been reported but at lower output power using a reversely biased SESAM very similar to the gain chip itself [24]. Modelocking of EP-VECSELs requires a design which is not only optimized for high cw output power but also for an optimal balance between electrical resistance, optical losses, dispersion and maximum achievable output power. In 2008, we presented a design of EP-VECSELs which are compatible with passive modelocking [25]. We present here a detailed characterization of the first fabrication of such EP-VECSELs. In addition, we discuss additional results obtained using EP-VECSELs fabricated by Philips U-L-M Photonics with designs for three different internal intermediate DBRs.

The paper is arranged as follows: first we describe the design of the EP-VECSELs fabricated at ETH Zurich (section II), followed by details on the MBE growth (section III) and on the fabrication of the chip (section IV). In section V we discuss the mode size limits for fundamental mode operation for these EP-VECSELs by analyzing the homogeneity of the current injection and comparing them with our numerical simulations. Afterwards the lasing performance of the fabricated EP-VECSELs and the power scaling are described (section VI) followed by a detailed discussion about the trade-off between good beam quality and high output power (section VII). These results are compared to M^2 measurements from EP-VECSELs fabricated at Philips U-L-M Photonics. Finally, we will summarize our results and give an outlook for the next generation of EP-VECSELs in section VIII.

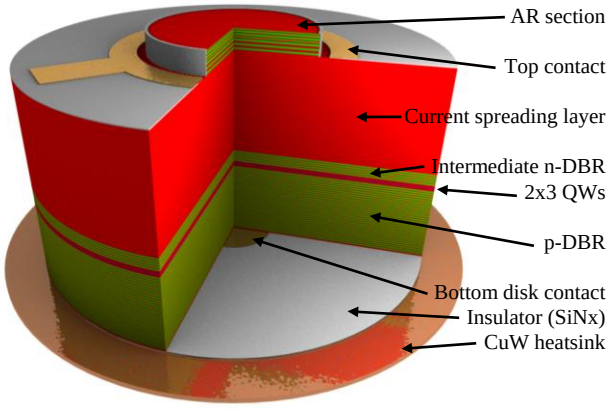

Fig. 1. Schematic of our EP-VECSEL design (not to scale). The final structure as shown here is without the initial GaAs substrate and soldered on a CuW heatsink.

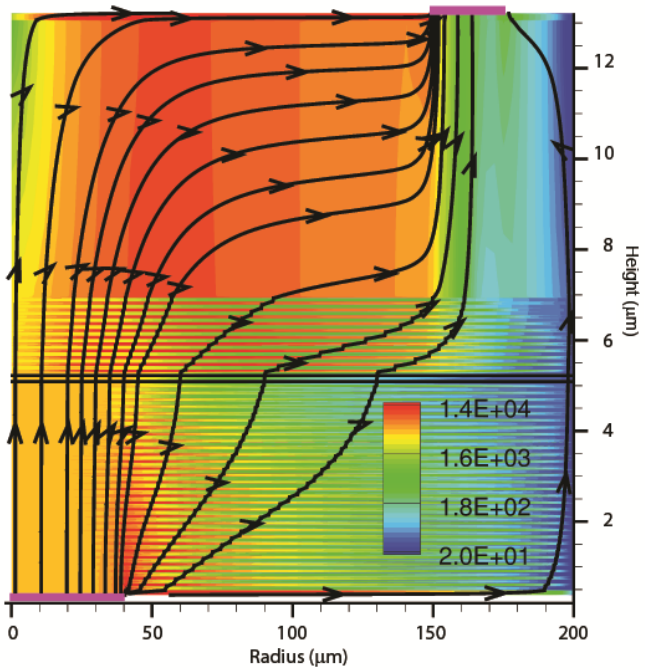

Fig. 2. EP-VECSEL simulation of the injected current in a radial symmetry (bottom disk contact Ø of 80µm). The color map of the current density is in A/cm^2, the black lines show current trajectories.

II. EP-VECSEL DESIGN

The design guidelines of our EP-VECSELs were previously discussed in [25]. Fig. 1 shows a not-to-scale 3D illustration of our EP-VECSEL chip which is stretched vertically for better visibility. The good confinement of the injected current to the center of the device is ensured by a p-doped DBR with a small bottom disk contact (BDC) and on top a thick current spreading layer (CSL) with a ring electrode. The low mobility of the holes in the p-DBR confines the carriers to the volume above the BDC and the high mobility of the electrons in the thick CSL allows their recombination in the center of the device [25, 26]. This is shown in more detail in Fig. 2 where the carrier transport was simulated in a device with a BDC diameter of 80 µm. The simulation tool used incorporates a coupled electro-opto-thermal model using microscopic carrier transport equations [26]. A thermionic emission model

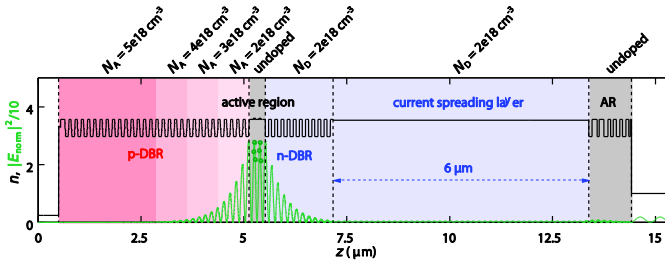

Fig. 3. Refractive index (black line) and electrical field (green line) profiles along the EP-VECSEL structure. The doping levels are indicated on top of the diagram. The active region consists of 2 groups of 3 InGaAs QWs spaced by 10 nm.

addresses abrupt hetero-interfaces [25]. As inputs, the device geometry and the material compositions are given. We have used standard parameter values that can be found in [27]. The color map of the current density shows three orders of magnitude and clearly confirms that the carriers are very well confined to the size of the BDC and that the CSL performs correctly. The BDC determines the mode size of the EP-VECSEL as demonstrated in section V, where the measured electroluminescence profiles are compared to our numerical model. As already discussed in [25], a low reflective intermediate n-DBR is inserted between the gain region and the CSL which reduces the cavity losses by decreasing the field strength in the doped top layers (Fig. 3). However, the sub-cavity between the two DBRs has a strong spectral filtering effect which reduces the bandwidth of the device. In addition, without an antireflection (AR) section on top of the device, the CSL would result in a second sub-cavity, deteriorating the device's performance.

An optical simulation for the field enhancements inside the structure is shown in Fig. 3. It was performed using a transfer matrix method [28]. The n-DBR enhances the field in the quantum wells (QWs) which compensates for the optical losses in the CSL, the n-doped DBR and p-doped DBR. The active region consists of two groups of three QWs which are arranged in adjacent field maxima.

The presented design should be suitable to be directly modelocked using an external SESAM as it is usually done with optically pumped ultrafast VECSELs [6]. For stable modelocked operation, the saturation energy of the absorber has to be lower than for the gain. The ratio can be controlled by the spot size on the SESAM, the field enhancement at the absorber position and the intrinsic absorber properties. For instance, quantum-dot (QD) saturable absorbers have lower saturation fluence than QW saturable absorbers [29-31]. For the generation of ultrashort pulses, the dispersion of the laser cavity needs to be optimized. Shortest pulse duration requires slightly positive dispersion to balance the nonlinear phase shift induced by strong semiconductor gain and absorber saturation [32].

III. Wafer Growth

The EP-VECSEL structure was grown by molecular beam epitaxy (MBE). We used a Veeco Applied Epi Gen III with two aluminum (Al) sources, two gallium (Ga) sources, one indium (In) source, a valved arsenic (As) cracking source, a silicon (Si) n-dopant source and a carbon tetrabromide (CBr4) p-dopant source. The EP-VECSEL structure was grown in reverse order to allow for substrate removal. The etch stop is a 300-nm thick $Al_{0.8}Ga_{0.2}As$ layer. The p-doped DBR has 30 AlAs/GaAs pairs, with doping levels of $(5, 4, 3, 2)\cdot10^{18}$ cm^{-3} for the DBR pairs (1-15, 16-20, 21-25, 26-30), respectively (Fig. 3). These different doping levels result in a lower electrical resistance of the EP-VECSELs. The electrical field is low in the bottom part of the mirror so higher doping does not significantly increase the optical losses.

In this first demonstration we applied 16 nm thick bandgap grading sections with five discrete $Al_{(x)}Ga_{(1-x)}As$ layers of intermediate compositions to smoothen the energy band discontinuity at the hetero-junction between AlAs and GaAs [33]. This results in precise layer thickness accuracies and close to a constant doping level over all layers within the bandgap grading sections. However, according to our simulations [25], a linear bandgap grading [34] would further reduce the electrical resistance in the p-DBR. However, linear bandgap grading with MBE is challenging and therefore we did not implement it in our first EP-VECSEL chip.

The low reflective intermediate n-DBR consists of high contrast AlAs/GaAs materials but does not have any bandgap grading sections because the decrease in electrical resistance of a graded n-DBR is minor compare to the actual resistance in the p-doped DBR [25]. The doping level in the n-DBR is kept constant at $2\cdot10^{18}$ cm^{-3}. The number of n-DBR pairs has been increased to 11 to ensure lasing in cw operation in this first demonstration.

The active region consists of two groups of three 7 nm thick InGaAs QWs which are placed in adjacent field maxima of the standing wave pattern of the laser and spaced by 10 nm of GaAs. The structure is designed for an operating wavelength of 965 nm and an internal temperature of ≈ 100°C. In order to center the maximum of the gain spectrum on the cavity resonance at high current injection we detune the QWs' luminescence peak wavelength by 25 nm to shorter wavelengths at room temperature [16]. The GaAs CSL is 6 µm thick and n-doped with a doping level of $2\cdot10^{18}$ cm^{-3}. Between the CSL and the AR section is an 150 nm thick contact layer n-doped up to $6\cdot10^{18}$ cm^{-3}. The top AlAs/GaAs AR section is undoped and the layer thicknesses were optimized for low reflectivity in an 8 nm bandwidth reflectivity using a Monte Carlo algorithm.

IV. EP-VECSEL Chip Fabrication

The wafer growth and the chip fabrication were realized in the FIRST cleanroom facility at ETH Zurich. Four series of 61 designs with different sizes were fabricated on a 14.5 x 12.5 mm^2 chip. The first fabrication step defines markers for wafer alignment. These are dry-etched completely through the structure to allow for alignment during backside and frontside processing. We use an inductively coupled

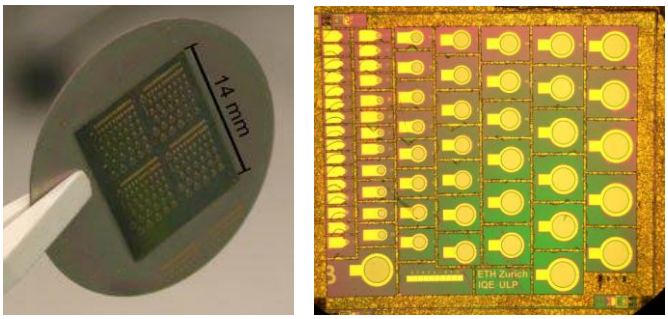

Fig. 4. Pictures of a realized EP-VECSEL chip and a zoom on a section with 61 EP-VECSELs. The distortion in the picture is caused by the microscope.

plasma (ICP) system with an Ar/Cl_2 recipe optimized to obtain deep and straight sidewalls. In a next step, a 300 nm thick silicon nitride (SiNx) layer is deposited in a plasma enhanced chemical vapor deposition (PECVD) system which acts as an electrical insulator (Fig. 1). The openings of the BDCs are produced by photolithography and dry etching in a reactive ion etching (RIE) system. Then, the entire semiconductor chip is coated with Ti/Pt/Au in order to form the bottom contacts. After that, the semiconductor chip is soldered onto a copper tungsten (CuW) carrier wafer which has a similar coefficient of thermal expansion (CTE) as GaAs. The CuW carrier wafer is 300 µm thick and 25 mm in diameter (left image in Fig. 4). The soldering employs a eutectic Au/Sn alloy and is performed with a wafer bonder at 340°C and 450 N/cm^2 to obtain a perfect joint. Next, the GaAs wafer is removed, first mechanically by lapping and then followed by wet etching in a citric acid hydrogen peroxide solution. The $Al_{0.8}Ga_{0.2}As$ etch stop layer ensures an optically flat surface. After the substrate removal, the markers for wafer alignment are clearly visible from the top. The AR section is then etched using ICP, stopping within the highly doped top contact layer. A second dry-etch step electrically and physically isolates the neighboring EP-VECSELs from each other by making deep trenches down to the insulating layer (right image in Fig. 4). The chip is again covered with SiNx. The top of the AR section and the electrical contacts are opened by photolithography and RIE etching. The side of the AR section is protected from oxidation by the remaining SiNx. The top electrical contacts are made with a lift-off process of an n-metallization stack of Ge/Au/Ge/Au/Ni/Au. The chip is finally annealed in a rapid thermal annealer (RTA) at 390°C to form ohmic contacts between the metallization and the semiconductor contact layer. Thanks to the CuW material, the lasers do not suffer from strain during this final annealing step.

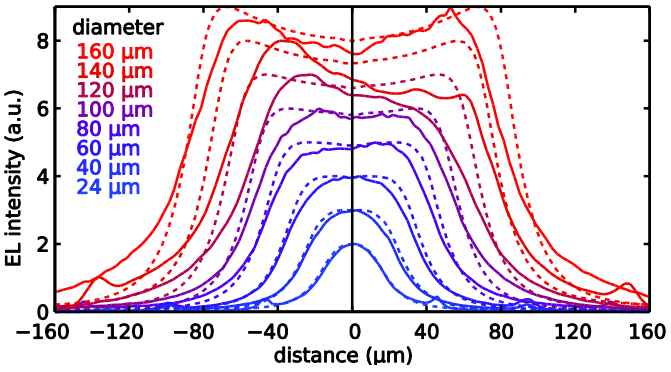

Fig. 5. Measured (solid lines) and simulated (dashed lines) electroluminescence (EL) profiles of EP-VECSELs with different bottom disk contact diameters.

V. Current Confinement in Large Devices.

Power scaling of EP-VECSELs in a fundamental laser beam mode (i.e. TEM_{00} beam) requires an efficient supply of carriers in the center of the active region even for large device diameters. The electroluminescence (EL) emission profile over the device area operated without external cavity is taken as a measure for the current injection into the gain. The confinement of the carriers in the active region was simulated using our coupled electro-opto-thermal model [25-27] (Fig. 2). The measured and simulated EL profiles of the EP-VECSELs for different BDC diameters are compared in Fig. 5. The measured EL profiles are in good agreement with the simulation results. For devices with diameters of up to 40 µm the emission resembles a Gaussian profile. Increasing the device diameter further, the profiles become increasingly flat-top-shaped and develop an intensity dip in the center of the device for diameters greater than 120 µm. For the devices with 120 and 140 µm BDC diameters, the measured EL profiles show asymmetries but the measured EL profile in the largest device (160 µm BDC diameter) is symmetric. The measured and simulated EL profiles in the largest device show a reasonable dip of ~11.5 % indicating that in our current device design, the complete active area can be efficiently pumped with sufficient homogeneity in the EL. Devices with BDC diameters up to 100 µm are favorable for TEM_{00} beams.

VI. Lasing Performance and Power Scaling.

We compared the lasing performance of EP-VECSELs with different aperture sizes at 3°C heatsink temperature in a simple straight cavity. The output coupler (OC) had a 25 mm radius of curvature and 10% transmission. The cavity length

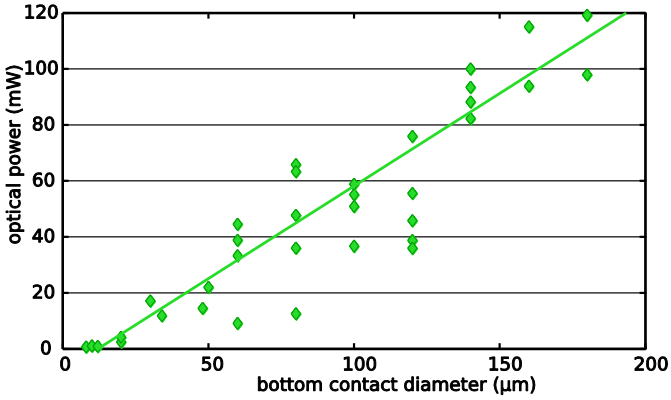

Fig. 6. Output power of EP-VECSELs in a straight cavity with a 10% transmission output coupler as function of the bottom disk contact diameter. The heatsink temperature was kept at 3°C.

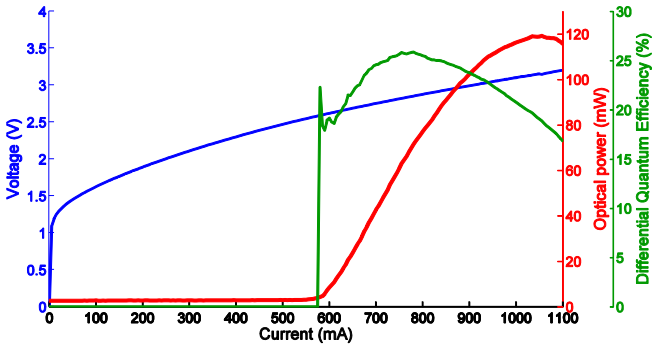

Fig. 7. LIV curves from an EP-VECSEL with a disk contact diameter of 180 µm, top contact diameter of 300 µm, using a 10% output coupler. The heatsink temperature was kept at 3°C.

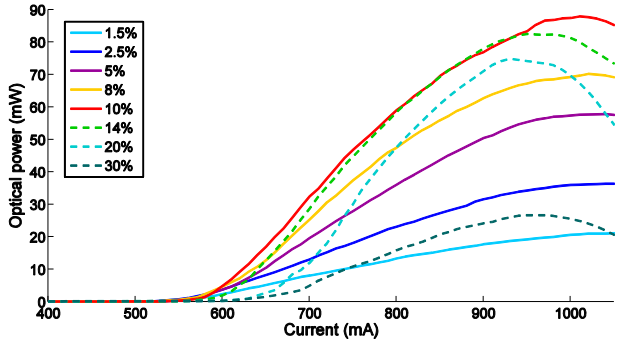

Fig. 8. LI curves from an EP-VECSEL with a disk contact diameter of 180 µm using different output coupler transmission. The heatsink temperature was kept at 20°C.

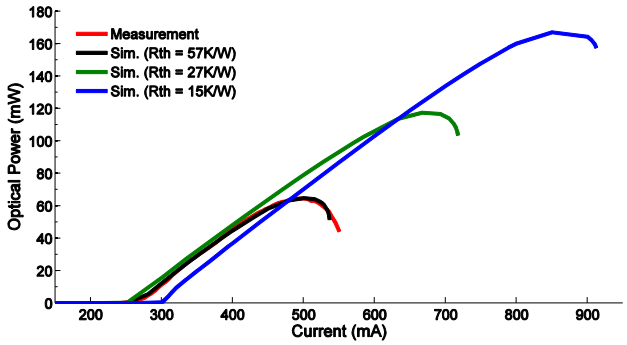

Fig. 9. Measured (red line) and simulated (black line) LI characteristics of an EP-VECSEL with a disk contact diameter of 80 µm and a 10% output coupler. The heatsink temperature is 3°C. The green and blue lines show a simulation with reduced thermal resistance.

of around 24.5 mm was optimized for maximum output power. In Fig. 6 the output power is plotted for 35 devices as a function of the BDC diameter. Despite slight variations among devices with identical active area, a linear increase of the output power as a function of the BDC diameter is evident, showing power scalability of the current design up to 120 mW. The roll-over for small devices occurs at substantially higher current densities than for larger devices. This gives some indication for thermal issues for the larger devices in our first demonstration because the power does not increase proportionally to the active area. This could be improved by reducing the heat dissipation by a lower electrical resistance of the devices or by use of a bottom heat sink with higher thermal conductivity. The employed CuW heatsink has a thermal conductivity of 200 $W \cdot K^{-1} \cdot m^{-1}$, which is two times lower than for copper and ten times lower than for diamond. A CTE matched alternative would be a composite silver-diamond heatsink with 650 $W \cdot K^{-1} \cdot m^{-1}$ thermal conductivity [35].

The light-current-voltage (LIV) curves of the EP-VECSEL delivering 120 mW of optical power using a 10% OC is shown in Fig. 7. It has a BDC diameter of 180 µm and a top contact electrode diameter of 300 µm. The thermal roll-over is obtained at ≈ 1 A. The differential quantum efficiency at 750 mA is about 25% and the wall-plug efficiency about 5%. A lower current threshold value could be expected but the 25 nm detuning of the QWs increases the lasing threshold [16]. The differential resistance of the laser presented in Fig. 7 is ≈ 1.5 Ω at lasing threshold.

In Fig. 8 the light-current (LI) curves of an EP-VECSEL with a BDC diameter of 180 µm are shown for different OC transmissions. The figure shows that the optimum transmission for high power would be ≈ 14% at 20°C. This value is much higher than what is typically used in OP-VECSELs because the EP-VECSEL intermediate n-DBR already transmits only 9% of the light in this initial realization.

The measured LI curves were also compared to our coupled electro-opto-thermal model [25-27]. In the simulation, the feedback from the OC is implemented as a flat mirror at a distance of only a few wavelengths away from the semiconductor surface. A comparison of theoretical and measured LI curves is shown in Fig. 9 for an EP-VECSEL with a BDC of 80 µm and 10% of output coupling. Threshold current, slope efficiency and thermal roll-over are in excellent agreement with the measurement. The internal temperature from self-heating has been extracted from the experimental wavelength shift versus pump current, and a thermal resistance of R_{th} = 57 K/W has been used in the simulation in order to give a comparable internal temperature rise from the calculation. In a second simulation, identical parameters have been used, only the thermal resistance has been reduced to 27 K/W and 15 K/W. This simulation is also shown in Fig. 9 with an increase in maximum output power to 117 mW and 170 mW respectively. The maximum output power in the current design is therefore limited by the strong internal heating as a result of an increased electrical and thermal resistance. The electrical resistance in the simulation is much lower compared to the experiment, and in this first device demonstration, it is caused by a not fully optimized fabrication process and a more highly resistive p-DBR with discrete $Al_{(x)}Ga_{(1-x)}As$ bandgap grading layers. Higher resistance leads to a higher temperature and an earlier roll-over limiting the maximum output power.

VII. EP-VECSEL BEAM QUALITY

The transverse mode quality of an EP-VECSEL is not only dependent on the EL profile, but also on various other parameters such as the external cavity, thermal lensing and aberrations. Furthermore, even for a perfect cavity design and a homogeneous current injection in the QWs, the transverse

TABLE I
BEAM QUALITY MEASUREMENTS ON PHILIPS U-L-M PHOTONICS EP-VECSELS

Internal reflectivity (%)	Output coupler transmission (%)	Output power (mW)	Beam quality M^2 value
90	2.5	3.1	11
90	5.0	22.2	8.8
90	10.0	34	2.6
82	2.5	17.3	1.4
82	5.0	15.1	1.1
82	10	10.6	1.5
71	1.5	7.5	1.2
71	2.5	8.2	1.1
71	5.0	no lasing	x

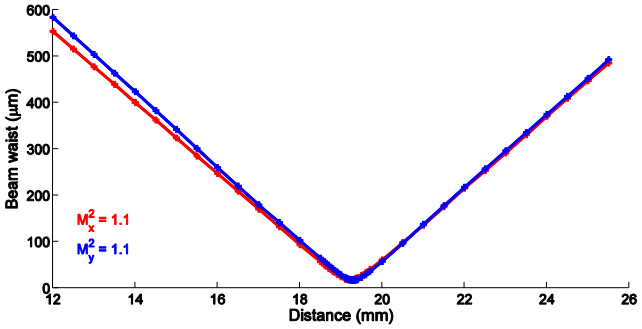

Fig. 10. Beam quality measurement of an EP-VECSEL from Philips U-L-M Photonics with 82% internal reflectivity and 5% transmission OC at 15 mW output power.

mode quality can be reduced by a relatively high reflectivity of the intermediate n-DBR. This is most likely the situation for this initial device demonstration. So far we only fabricated one series of EP-VECSELs with a 91% reflectivity of the intermediate n-DBR to assure lasing. From a device with a BDC diameter of 80 µm we obtained ≈ 30 mW output power with an M^2 value of 3.6 in a straight cavity using an OC with 10% transmission and 25 mm radius of curvature. A nearly fundamental transverse mode was obtained by using an aperture, however, the output power in this case was less than 10 mW.

To experimentally evaluate the influence of the n-DBR reflectivity, we used a different set of EP-VECSELs that were produced at Philips U-L-M Photonics. These devices were realized with 13, 11 and 9 intermediate n-DBR pairs corresponding to three different internal reflectivities of 90%, 82% and 71%. The diameter of the electrically pumped area for all devices was 100 µm. One difference to the ETH design is a thicker CSL (60-80 µm at a doping level of $0.5\text{-}1.0\cdot10^{18}$ cm^{-3}), introducing more optical losses due to free carrier absorption. Therefore, the maximum achievable output power is reduced. Although there are further design differences, we can consider that the general relations between internal reflectivity, output power and achievable transverse beam quality are similar. We characterized the devices in a straight cavity using OCs with different transmission values from 1.5 to 10% and radius of curvature of 15 mm or 25 mm. In order to optimize beam quality the laser cavity is designed taking into account the strong thermal lens of such type of lasers [16]. The focal length on the EP-VECSELs due to carrier and thermal effects has been estimated to be 2 mm at high injection current. The different combinations of laser cavities with the resulting M^2 values and output power levels are listed in Table 1. For the device with 90% reflectivity, which is a similar design as presented in the previous sections, we clearly observe that beam quality and power level increase when we increase the OC transmission from 2.5% to 10%. The best M^2 value obtained for this device was 2.6 at 34 mW of output power. For the other samples with lower internal reflectivity of 82% and 71%, we could obtain a nearly fundamental transverse mode of all tested output couplers ($M^2 < 1.5$). The maximum output powers were 17.2 mW and 8.2 mW, respectively. All measurements were performed close to the thermal roll-over. High current injection does therefore not introduce large aberrations. In Fig. 10, we show the measurement of the 82% sample at 5% output coupling, for which 15 mW were obtained at $M^2 = 1.1$. The measurements demonstrate that a correctly balanced field enhancement and output coupling is necessary to combine good beam quality and high output power. A higher reflectivity of the intermediate n-DBR reduces the penalty of the losses in the external cavity, but also reduces the mode control of the external curved OC and therefore leads to a deteriorated beam quality.

VIII. CONCLUSION AND OUTLOOK

We presented a first series of EP-VECSELs of different sizes based on our design guidelines published in [25]. We described the exact design used for the fabrication, details on the growth of the semiconductor structure, details on the fabrication process, the lasing performance and a comparison to our coupled electro-opto-thermal model. The presented and discussed experimental and simulation results could reveal and quantify all the relevant trade-offs for power scaling with increased mode sizes. The challenge for high-power modelocked EP-VECSELs is first to get high power levels by scaling the devices laterally keeping a homogeneous electrical pumping and second to balance the competing requirements of low electrical resistance, low optical losses and controlled dispersion while maintaining fundamental mode operation for stable modelocking. For the EP-VECSELs presented here, the entire active area can be pumped efficiently with sufficient homogeneity even for large diameter devices. This is in very good agreement with the simulation results. Devices with BDC diameters of up to 100 µm are favorable for TEM_{00} output beams. Promising output power levels were obtained in continuous wave and could scale the power up to 120 mW despite a higher resistance in the p-DBR than expected. Our simulations predict for an optimized device with only 80 µm diameters output power levels of ≈ 170 mW.

For passive modelocking, it is important to operate the device in a nearly single transverse mode, because the presence of higher order modes can destabilize the pulses. We showed that the choice of the internal reflection of the intermediate n-DBR has a strong influence on the beam quality. A high reflectivity of the intermediate n-DBR yields

high gain, but also reduces the mode control of the external cavity. In this initial device demonstration, the internal reflection from the intermediate n-DBR was ≈ 90%, which limited the achievable beam quality to M^2 values above 3 for operation at >30 mW. Using different EP-VECSEL chips from U-L-M Photonics, we could experimentally study the influence of the intermediate n-DBR reflectivity on the beam quality and output power. We showed that for maximum output power and good beam quality, an intermediate n-DBR with ≈ 80% reflectivity appears optimal. Based on the presented investigations we expect that the next generation of EP-VECSELs with improved designs will result in higher output powers with good beam quality to support modelocking with an external low saturation fluence QD-SESAM.

REFERENCES

[1] U. Keller, "Recent developments in compact ultrafast lasers," *Nature*, vol. 424, pp. 831-838, 14.08. 2003.

[2] E. Murphy, "The semiconductor laser: Enabling optical communication," *Nat Photon*, vol. 4, pp. 287-287, 2010.

[3] J. J. Plant, *et al.*, "250 mW, 1.5 µm monolithic passively modelocked slab-coupled optical waveguide laser," *Opt. Lett.*, vol. 31, pp. 223-225, 2006.

[4] T. Schlauch, *et al.*, "High peak power femtosecond pulses from modelocked semiconductor laser in external cavity," *Electronics Letters*, vol. 44, pp. 678-679, 2008.

[5] M. Kuznetsov, *et al.*, "High-Power (>0.5-W CW) Diode-Pumped Vertical-External-Cavity Surface-Emitting Semiconductor Lasers with Circular TEM00 Beams," *IEEE Photon. Technol. Lett.*, vol. 9, pp. 1063-65, 1997.

[6] U. Keller and A. C. Tropper, "Passively modelocked surface-emitting semiconductor lasers," *Phys. Rep.*, vol. 429, pp. 67-120, June 2006.

[7] U. Keller, *et al.*, "Semiconductor saturable absorber mirrors (SESAMs) for femtosecond to nanosecond pulse generation in solid-state lasers," *IEEE J. Sel. Top. Quantum Electron.*, vol. 2, pp. 435-453, 1996.

[8] D. J. H. C. Maas, *et al.*, "Vertical integration of ultrafast semiconductor lasers," *Appl. Phys. B*, vol. 88, pp. 493-497, 2007.

[9] A.-R. Bellancourt, *et al.*, "Modelocked Integrated External-Cavity Surface Emitting Laser (MIXSEL)," *IET Optoelectronics*, vol. Vol. 3, pp. pp. 61-72, 2009.

[10] B. Rudin, *et al.*, "High-power MIXSEL: an integrated ultrafast semiconductor laser with 6.4 W average power," *Opt. Express*, vol. 18, pp. 27582-27588, 2010.

[11] A. H. Quarterman, *et al.*, "A passively mode-locked external-cavity semiconductor laser emitting 60-fs pulses," *Nat. Photonics*, vol. 3, pp. 729-731, Dec 2009.

[12] P. Klopp, *et al.*, "Mode-Locked InGaAs-AlGaAs disk laser generating sub-200-fs pulses, pulse picking and amplification by a tapered diode amplifier," *Opt. Express*, vol. 17, pp. 10820-10834, 2009.

[13] A. Aschwanden, *et al.*, "2.1-W picosecond passively mode-locked external-cavity semiconductor laser," *Opt. Lett.*, vol. 30, pp. 272-274, 2005.

[14] A. H. Quarterman, *et al.*, "Active stabilisation and timing jitter characterisation of sub-500 fs pulse passively modelocked VECSEL," *Electronics Letters*, vol. 44, pp. 1135-1137, 2008.

[15] J. G. McInerney, *et al.*, "High-power surface emitting semiconductor laser with extended vertical compound cavity," *Electron. Lett.*, vol. 39, pp. 523-525, 20th March 2003 2003.

[16] J. G. McInerney, *et al.*, "Novel 980-nm and 490-nm light sources using vertical cavity lasers with extended coupled cavities," in *SPIE 2003*, Brugge, Belgium, 2003, pp. 21-31.

[17] S. Illek, *et al.*, "Vertical-External-Cavity Surface-Emitting Laser With Monolithically Integrated Pump Lasers," *IEEE Photon. Technol. Lett.*, vol. 19, pp. 1952-1954, 2007.

[18] W. Diehl, *et al.*, "High power semiconductor disk laser with monolithically integrated pump lasers," in *SPIE Photonics Europe*, Strasbourg, France, 2008, pp. 699711-7.

[19] M. E. Kurdi, *et al.*, "Room-temperature continuous-wave laser operation of electrically-pumped 1.55 µm VECSEL," *Electr. Lett.*, vol. 40, pp. 671-672, 2004.

[20] A. Bousseksou, *et al.*, "Fabrication and characterization of 1.55 um single transverse mode large diameter electrically pumped VECSEL," *Optical and Quantum Electronics*, vol. 38, pp. 1269-1278, 2006.

[21] A. Harkonen, *et al.*, "2.34 um electrically pumped VECSEL with buried tunnel junction," in *SPIE Photonics Europe*, Brussels, Belgium, 2010, pp. 772015-7.

[22] W. Jiang, *et al.*, "Electrically pumped mode-locked vertical-cavity semiconductor lasers," *Opt. Lett.*, vol. 18, pp. 1937-1939, 1993.

[23] K. Jasim, *et al.*, "Passively modelocked vertical extended cavity surface emitting diode laser," *Electron. Lett.*, vol. 39, pp. 373-375, 2003.

[24] K. Jasim, *et al.*, "Picosecond pulse generation from passively modelocked vertical cavity diode laser at up to 15 GHz pulse repetition rate," *Electron. Lett.*, vol. 40, pp. 34-35, 2004.

[25] P. Kreuter, *et al.*, "On the Design of Electrically-Pumped Vertical-External-Cavity Surface-Emitting Lasers," *Appl. Phys. B*, vol. 91, pp. 257-264, 2008.

[26] B. Witzigmann, *et al.*, "Physics and Simulation of Vertical-Cavity Surface-Emitting Lasers," *Journal of Computational and Theoretical Nanoscience*, vol. 5, pp. 1058-1071, 2008.

[27] J. Piprek, Ed., *Optoelectronic Devices: Advanced Simulation and Analysis*. Springer, 2005.

[28] J. Chilwell and I. Hodgkinson, "Thin-films field-transfer matrix theory of planar multilayer waveguides and reflection from prism-loaded waveguides," *J. Opt. Soc. Am. A*, vol. 1, pp. 742-753, 1984.

[29] G. J. Spühler, *et al.*, "Semiconductor saturable absorber mirror structures with low saturation fluence," *Appl. Phys. B*, vol. 81, pp. 27-32, 2005.

[30] D. J. H. C. Maas, *et al.*, "Growth parameter optimization for fast quantum dot SESAMs," *Opt. Express*, vol. 16, pp. 18646-18656, 2008.

[31] A.-R. Bellancourt, *et al.*, "Low Saturation Fluence Antiresonant Quantum Dot SESAMs for MIXSEL integration," *Opt. Express*, vol. 17, pp. 9704-9711, 2009.

[32] M. Hoffmann, *et al.*, "Experimental verification of soliton-like pulse-shaping mechanisms in passively mode-locked VECSELs," *Opt. Express*, vol. 18, pp. 10143-10153, 2010.

[33] G. W. Pickrell, *et al.*, "Compositional grading in distributed Bragg reflectors, using discrete alloys, in vertical-cavity surface-emitting lasers," *Journal of Crystal Growth*, vol. 280, pp. 54-59, 2005.

[34] M. Hong, *et al.*, "A simple way to reduce series resistance in p-doped semiconductor distributed Bragg reflectors," *Journal of Crystal Growth*, vol. 111, pp. 1071-1075, 1991.

[35] M. Faqir, *et al.*, "Novel packaging solutions for GaN power electronics: Silver-diamond composite packages," in *The International Conference on Compound Semiconductor Manufacturing Technology*, Portland, Oregon, USA, 2010, p. 307.

Yohan Barbarin graduated in 2002 from the Marseille national higher school in physics and engineering (ENSPM), nowadays integrated in the École Centrale Marseille, France. Yohan joined afterwards the Opto-Electronic Devices group at COBRA Research Institute, Eindhoven University of Technology, The Netherlands. He developed integrated modelocked semiconductor laser sources for 160–640 Gbit/s optical time-domain multiplexed (OTDM) applications and obtained the Ph.D. degree in 2006. In 2007, Yohan joined the Ultrafast Laser Physics group at ETH Zurich, Switzerland. He is currently working as a researcher on the development of high power electrically pumped vertical external cavity surface emitting lasers (VECSELs) and the modelocking of such lasers with quantum-dot semiconductor saturable absorber mirrors (SESAMs).
Dr. Barbarin is a Member of the IEEE.

Martin Hoffmann was born in Dessau, Germany, on October 15, 1979. He received his Diploma in physics in 2007 from the Federal Institute of Technology, ETH Zurich, in Zurich, where he is currently working towards the Ph.D. degree in Prof. Ursula Keller's group (Ultrafast Laser Physics). His current research interests include semiconductor saturable absorber mirror modelocked quantum dot and quantum well based vertical external cavity surface emitting lasers, both optically and electrically pumped. Mr. Hoffmann is a member of the OSA.

Wolfgang Pallmann was born in Nürnberg, Germany, on June 9, 1983. He studied at Friedrich-Alexander-University Erlangen-Nürnberg, where he obtained his diploma in electrical engineering in 2009.At present he is working on his Ph.D. degree in the group of Prof. Ursula Keller (Ultrafast Laser Physics) at ETH Zürich. His main research interest is the development of ultrafast electrically and optically pumped vertical external cavity surface emitting lasers.

Imad Dahhan was born in Cardiff, UK in 1982. He received his Diploma in Electrical Engineering in October 2009 from the the Technical University of Munich, Germany. He is now working towards the Ph.D. degree at the Ultrafast Laser Physics group, Institute for Quantum Electronics, ETH Zurich, and is a guest scientist at the Computational Electronics and Photonics group, University of Kassel, Germany. His research interests are in the fields of semiconductor and laser physics, with a focus on numerical modeling of optoelectronic devices, passively modelocked VECSELs and the nonlinear dynamics of pulse generation.

Philipp Kreuter was born in Germany, in 1978. He studied electrical engineering at the Technical University of Munich, Germany, the 'Ecole Nationale Superieure de l'Aeronautique et de l'Espace in Toulouse, France, and the Universitat Politecnica de Valencia, Spain. He received the B.Sc. and Dipl.-Ing. degrees in Electrical Engineering from the Technical University of Munich, in 2004 and 2005 respectively. In October 2005, he joined the Integrated Systems Laboratory of the Swiss Federal Institute of Technology Zurich (ETHZ) from which he received the Ph.D. degree, in 2010. His research interests are in the field of numerical modeling of optoelectronic devices with a focus on the highly nonlinear and dynamic processes in modelocked VECSELs.

Michael Miller was born in Heidenheim, Germany, on February 05, 1971. He studied Physics at University of Ulm and received the Diploma in 1997. He was member of the Optoelectronics Department at University of Ulm in the group of Prof. Ebeling working on high-power VCSEL where he obtained his Ph.D. in 2002. Currently he is working in the Research and Development Department of Philips Technologie GmbH, U-L-M photonics, as project manager in the field of high-power VCSEL.

Johannes Baier studied physics at the University of Bayreuth, Germany, where he received his diploma in 1994. After obtaining his Ph.D. in 1999 he joined the Philips Research Laboratories in Aachen, initially working on high intensity discharge and projection lamps. Since several years, however, his research interests have focused on the design and optimization of EP-VCSELs.

Holger Moench joined Philips Research in 1991 after his Ph.D. in High Energy Physics at the RWTH Aachen. He has been working on various high brightness and highly efficient light sources and their application in optical systems. As a "research fellow" he is now responsible for the research on lasers and their application in projection systems, material processing and optical sensors. His current research interests include the integration of semiconductors and optics, the design of advanced VCSEL structures and new applications for optoelectronic systems. He has published more than 70 papers and holds or applied for more than 80 patents.

Matthias Golling was born in Sulz, Germany, on May 20, 1971. He received the Diploma in electrical engineering in 1997, and the Ph.D. degree in engineering in 2004, both from University of Ulm, Ulm, Germany. He is currently leading the MBE (molecular beam epitaxy) activities of the Ultrafast Laser Physics group at ETH Zurich, Zurich, Switzerland.
His current research interests include the design and epitaxy of lasers and saturable absorbers.

Thomas Sudmeyer studied Physics in the University of Hanover and the Ecole Normale Supérieure, Paris. In 1999, during a six month EU research fellowship at the Institute of Photonics in Glasgow, he became interested in high power modelocked lasers. In 2003, he obtained a Ph. D. from ETH Zurich for research on the first modelocked thin-disk lasers and the realization of novel nonlinear systems. From 2003 to 2005, he developed industrial laser solutions such as high power 266-nm lasers at the Photonics Research Department of Sony Corporation, Tokyo. Since 2005, he is head of the ultrafast laser section in Ursula Keller's group at ETH. His current scientific interests include femtosecond thin disk lasers, multi-gigahertz repetition rate lasers, modelocked VECSELs and MIXSELs, and their applications in nonlinear optics and high field science. He is author of more than 40 papers in international peer-reviewed journals, two book chapters, several patents are pending. He has been the coordinator of the FP6 European Project MULTIWAVE. He serves the optical community in various conference committees and as associate editor for Optics Express.

Bernd Witzigmann received the diploma degree in Physics from the University of Ulm, Germany, and the Ph.D. degree (with honors) in technical sciences from the Swiss Federal Institute of Technology (ETH), Zürich, Switzerland, in 1996 and 2000, respectively. He then joined Bell Laboratories, Murray Hill, NJ, as a Member of technical staff. In October 2001, he joined the Optical Access and Transport Division of Agere Systems, Alhambra, CA. In 2004, he was appointed Assistant Professor at ETH Zurich in Switzerland. Since 2008, he has been Professor at the University of Kassel and head of the Computational Electronics and Photonics Group.
His research interests focus on computational optoelectronics, process and device design of semiconductor photonic devices, microwave components, and electromagnetics modeling for nanophotonics. Dr. Witzigmann is a Member of the IEEE and SPIE.

Ursula Keller joined ETH as professor of physics in 1993. She received the Ph.D. in Applied Physics from Stanford University in 1989 and the Physics "Diplom" from ETH in 1984. She was a Member of Technical Staff (MTS) at AT&T Bell Laboratories in New Jersey from 1989 to 1993. Her research interests are exploring and pushing the frontiers in ultrafast science and technology: ultrafast solid-state and semiconductor lasers, frequency comb generation and stabilization, attosecond pulse generation and science using high harmonic generation. She has published more than 300 peer-reviewed journal papers and 11 book chapters and she holds or applied for 17 patents. She received the OSA Fraunhofer/Burley Prize in 2008, the Philip Morris Research Award in 2005, the first-placed award of the Berthold Leibinger Innovation Prize in 2004, and the Carl Zeiss Research Award in 1998. She is an OSA Fellow and an elected foreign member of the Royal Swedish Academy of Sciences and the German Academy Leopoldina.